CHINESE OPTICS LETTERS

Vol. 19, No. 1 | January 2021

Demonstration of joule-level chirped pulse amplification based on tiled Ti:sapphire amplifier

Keyang Liu (刘柯阳)[1,2,3], Yanqi Liu (刘彦祺)[1*], Yunhai Tang (唐云海)[1], Junchi Chen (陈骏驰)[1], Cheng Wang (王 乘)[1], Xingyan Liu (刘星延)[1,2,3], Xiaobin Wang (王晓斌)[1], Yingbin Long (龙应斌)[1], Yi Xu (许 毅)[1], Yujie Peng (彭宇杰)[1], Xiaoming Lu (陆效明)[1], Zhengzheng Liu (刘征征)[1], and Yuxin Leng (冷雨欣)[1,2,4**]

[1] State Key Laboratory of High Field Laser Physics, Shanghai Institute of Optics and Fine Mechanics, Chinese Academy of Sciences, Shanghai 201800, China

[2] School of Physical Science and Technology, ShanghaiTech University, Shanghai 200031, China

[3] University of Chinese Academy of Sciences, Beijing 100049, China

[4] CAS Center for Excellence in Ultra-intense Laser Science, Shanghai 201800, China

*Corresponding author: liuyanqi@siom.ac.cn

**Corresponding author: lengyuxin@mail.siom.ac.cn

Received July 7, 2020 | Accepted August 28, 2020 | Posted Online November 20, 2020

A novel tiled Ti:sapphire (Ti:S) amplifier was experimentally demonstrated with >1 J amplified chirped pulse output. Two Ti:S crystals having dimensions of 14 mm× 14 mm× 25 mm were tiled as the gain medium in a four-pass amplifier. Maximum output energy of 1.18 J was obtained with 2.75 J pump energy. The energy conversion efficiency of the tiled Ti:S amplifier was comparable with a single Ti:S amplifier. The laser pulse having the maximum peak power of 28 TW was obtained after the compressor. Moreover, the influence of the beam gap on the far field was discussed. This novel tiled Ti:S amplifier technique can provide a potential way for 100 PW or EW lasers in the future.

Keywords: Ti:sapphire crystal; tiled Ti:sapphire amplifier; chirped pulse.
DOI: 10.3788/COL202119.011401

1. Introduction

Ultrashort and ultraintense laser systems contribute to many significant applications, such as laser-plasma electron and ion accelerations[1,2], fast ignition[3], and astrophysics in laboratory[4]. With the invention of the chirped pulse amplification (CPA) technique[5], many ultrashort and ultraintense laser systems have been built worldwide. In recent years, several 10-PW-level high-power laser systems are under construction[6], such as the Shanghai Superintense Ultrafast Laser Facility (SULF) 10 PW at the Shanghai Institute of Optics and Fine Mechanics (SIOM)[7,8], the high-power laser system that delivers two 10 PW laser beams at the Extreme Light Infrastructure Nuclear Physics (ELI-NP)[9], and Apollon 10 PW laser[10], which are all based on the Ti:sapphire (Ti:S) amplifier. For these 10-PW-level Ti:S laser systems, Ti:S crystals with more than 200 mm diameter aperture are needed. However, when the aperture of the Ti:S crystal is more than 200 mm, the crystal becomes expensive and good-optical-quality crystals become extremely difficult to grow. Meanwhile, for >200 mm Ti:S crystals with high pump energy, the parasitic laser (PL) and the transverse amplified spontaneous emission (TASE) severely limit the signal gain and energy extraction efficiency. A series of techniques for suppressing PL and TASE have been reported, such as using the matched index liquid and lightly doped crystal and the temporal dual-pulse pump technique[11–13]. However, the existing Ti:S crystals and the techniques for suppressing PL and TASE cannot meet the requirements for future ultrashort and ultraintense laser systems of more than 10 PW. Moreover, coherent beam combination (CBC) has been regarded as a technique to improve the output power of laser systems with several small crystals[14,15]. But, accurate CBC in the time domain and space domain for femtosecond-class pulse duration and micron-class focused spot is very difficult and complex. Until now, the CBC technique has not been used in 10-TW-level laser systems[16].

In recent years, optical tiling technology has been used in many research activities, such as larger-aperture telescopes (tiling several small mirrors together to make a large mirror achieve the same properties as a single mirror)[17], tiling large-aperture nonlinear optical crystals[18], and tiling gratings[19]. The tiled Ti:S technique, known as one of the CBC techniques, is easier and simpler for controlling dispersion, synchronization, and focused spot. In a previous study, the tiled Ti:S crystal technology based on the CPA laser system had been studied[20], and the synchronization feasibility had been previously demonstrated with lower energy. Therefore, for petawatt (PW)-level Ti:S CPA

laser systems, the amplifier based on tiled Ti:S crystal technology should be a potential way to achieve higher peak power output and suppress PL with small crystals.

In this study, we experimentally demonstrated the feasibility of a new type of tiled Ti:S four-pass amplifier based on a 10-TW-level CPA laser. An amplified output energy of 1.18 J with pump energy of 2.75 J corresponding to an energy conversion efficiency of 35.3% was obtained. After the compressor, a pulse laser of the maximum peak power with 28 TW from the tiled Ti:S amplifier was finally achieved. Moreover, the effect of beam gap on the far-field spatial profile was discussed.

2. Experiment

The overall experimental setup is shown in Fig. 1. The femtosecond Ti:S laser oscillator generated 12 fs pulses at 80 MHz repetition rate. Then, the pulse duration was stretched to 2.4 ns via an all-reflective Öffner-type stretcher with output energy of 5 nJ. After a Ti:S regenerative amplifier and two multipass Ti:S amplifiers, a soft-edge double-array square diaphragm was used to spatially acquire the double-array square beam to fit the mounting structure of crystals [Figs. 2(a) and 2(b)]. Therefore, the initial parameters of the two signal beams should be the same, including the relative time delay and phase. The whole energy of the double-array square beams was 209 mJ with a double size

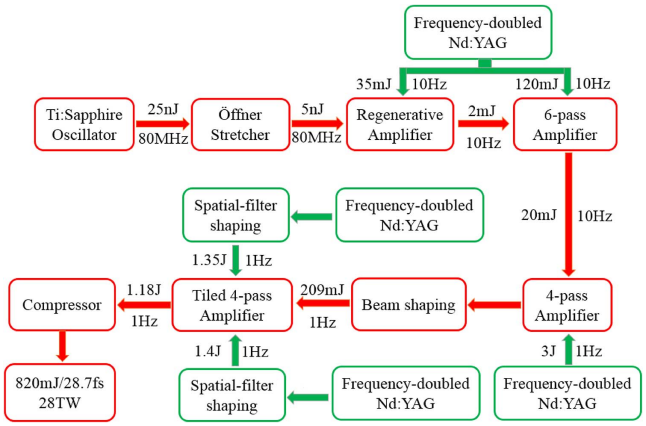

Fig. 1. Overall experimental setup.

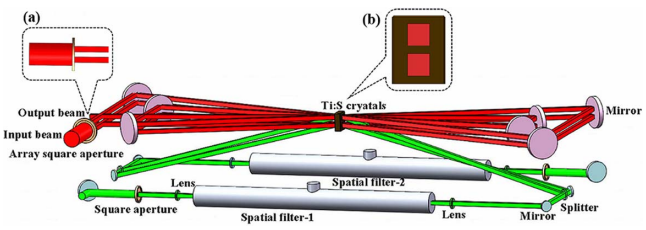

Fig. 2. Tiled Ti:S four-pass amplifier scheme. The red line is the signal beam, while the green line is the pump beam. The insets show (a) the signal beam shaping and (b) the mounting structure of the Ti:S crystals.

of 10 mm× 10 mm before the four-pass tiled Ti:S amplifier, which was pumped by 2.75 J pumping lasers. Finally, a grating compressor was used to compress the amplified chirped pulses simultaneously.

The simplified layout of the tiled Ti:S four-pass amplifier is presented in Fig. 2. Since the redesign of the tiled Ti:S four-pass amplifier, the pump beams and signal beams were situated on a different optical plane, and the tiled Ti:S crystals were installed in the vertical array direction (upper and lower), as shown in Fig. 2(b). The pump beam was shaped into a square having a 10 mm× 10 mm size to fit the appearance and aperture of the tiled Ti:S crystals using a spatial filter. Then, the pump pulse was divided into two lasers with approximately the same energy using a beam splitter and injected into one side of the tiled Ti:S crystals. Meanwhile, similar pump lasers were injected into another side of the tiled Ti:S crystals. Even more remarkably, the two tiled Ti:S crystals had the same length, width, and thickness, having dimensions of 14 mm × 14 mm × 25 mm (the crystals were processed together, including cutting, orientation of the optical axis, polishing, and coating), and the optical axis error of the two Ti:S crystals should be $< 1°$ to avoid possible issues including spectral modulation[20]. In addition, the gap of the tiled crystals was ~6 mm. To weaken the diffraction effect from the square aperture of the Ti:S crystals, a soft-edge square diaphragm with a double size of 12 mm × 12 mm was used to attach to one side of the mounting rack of the Ti:S crystals.

The following Frantz–Nodvik (F–N) function was used to simulate the output energy of the tiled Ti:S four-pass amplifier[21,22]:

$$\Delta N = N_T \left\{ 1 - \frac{1}{1 - \exp(-\alpha_p z)[1 - \exp(J_p/J_s)]} \right\}, \tag{1}$$

$$G_0 = \exp(J_{\text{sto}}/J_s), \tag{2}$$

$$J_{\text{out}} = J_s \ln\{1 + G_0[\exp(J_{\text{in}}/J_s) - 1]\}, \tag{3}$$

where ΔN is the inverted population density, N_T is the Ti^{3+} particle concentration, α_p is the pump absorption coefficient, J_p is the pump energy density, J_s is the saturation energy flux, J_{sto} is the stored energy per unit volume, G_0 is the small-signal gain, and J_{out} is the output energy flux.

As shown in Fig. 3, the experimental and simulated results of the output energy coincide well with the same input energy. Due to the energy limitation of the pump and the input signal laser, the amplifier was not saturated finally. A maximum amplified output energy of 1.18 J with an input signal energy of 209 mJ and a pump energy of 2.75 J was obtained, corresponding to approximately five times gain and 35.3% energy conversion efficiency, which was similar to a single Ti:S amplifier.

To prove that the tiled Ti:S amplifier would not introduce the spectral modulation, the spectrum obtained in Fig. 4 illustrates the laser spectral evolution of the input and output of the tiled Ti:S amplifier. It clearly shows that the spectral modulation in

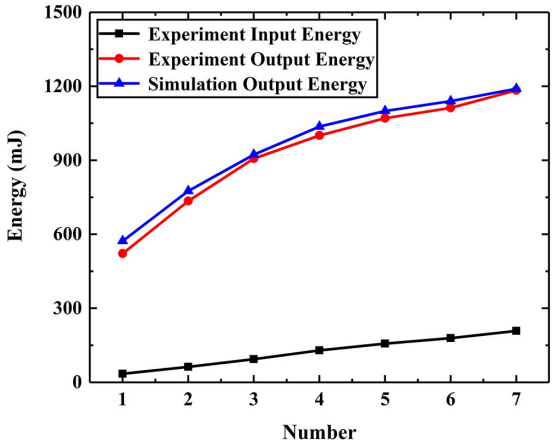

Fig. 3. Experimental and simulated results of the output energy of the tiled Ti:S amplifier at the same input energy.

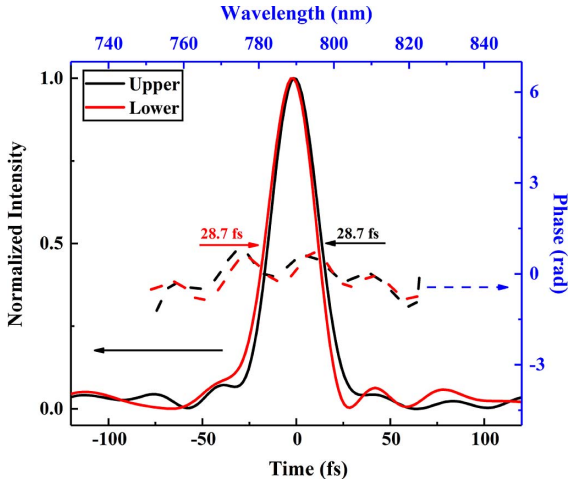

Fig. 5. Measured duration and spectral phase of compressed pulses.

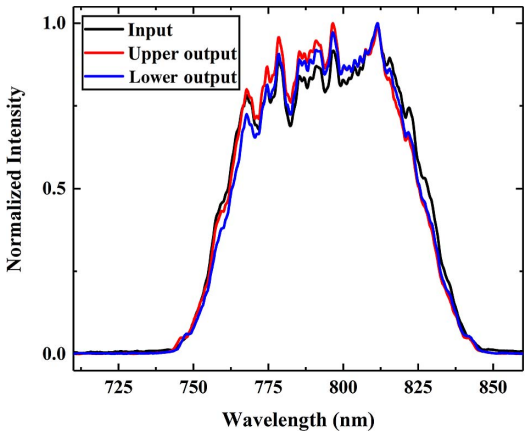

Fig. 4. Laser spectral evolution of the input and output of the tiled Ti:S amplifier.

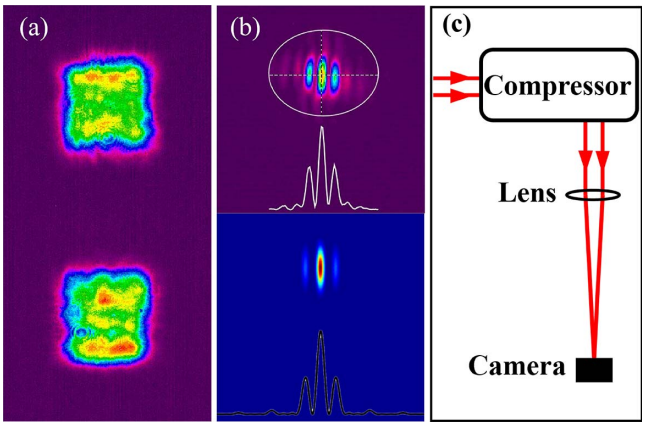

Fig. 6. Spatial profile of the output beam of the tiled Ti:S amplifier. (a) The near-field spatial profile. (b) The far-field spatial profile after the compressor: the experimental (upper) and the simulated (lower) results. (c) The measurement scheme.

the upper and lower output spectra hardly exists. Moreover, the spectral width of the upper and lower Ti:S crystals could be identified as uniform to support a 22.5 fs transform-limited (TL) pulse.

The amplified pulse was compressed through the optimized compressor consisting of two 1480 grooves/mm gold-coated reflective gratings. As shown in Fig. 5, the duration of the compressed pulse with the 28.7 fs FWHM was obtained by a Wizzler device (Fastlite). Meanwhile, the residual high-order dispersion brings the aberration for the spectral phase and pulse profile. Due to the 70% compressor efficiency, the output energy of compressed pulse was 820 mJ, corresponding to the maximum peak power of 28 TW.

The near-field spatial profile of output beam is presented in Fig. 6(a). The diffraction effect of the square aperture of the Ti:S crystals can cause slight modulation in the near-field spatial profile, which could be decreased by further enlarging the scale of the crystals. Furthermore, a convex lens with a focal length of 1 m was used to obtain the far-field spatial profile of the output beam after the compressor, and the pictures are the experimental (upper) and simulated (lower) results, as shown in Figs. 6(b) and 6(c). According to the expression of the combining efficiency[23], in the practical experiment, the combining efficiency of the two beams was 78.2%.

It is noted that the side peak intensity of the far-field spatial profile of the output beams is about 50% of the main peak intensity, as shown in Fig. 6(b), and that this will decrease the focused intensity and combining efficiency. This phenomenon appears because the output beam gap (the Ti:S crystals have the effective optical aperture of 70% loading the output beam gap of ~10 mm) indicated in Fig. 6(a) is too large compared with the 10 mm beam size. According to the numerical simulation, the main peak intensity and combining efficiency will increase when the output beam gap is reduced. Therefore, we can design

an adjusting scheme to decrease the beam gap and use the spatial filter to remove the side lobe of the far-field spot in future practical applications. In addition, due to the adoption of the same crystal thickness and beam transmission systems, such as mirrors and gratings, the relative spatial phase, wavefront, and combining efficiency are controllable in the tiled Ti:S technique. However, the time jitter problem of the conventional CBC technique can cause wavefront jitter[24]. Therefore, the tiled Ti:S technique is more beneficial to the compensation of the wavefront than the conventional CBC technique.

3. Conclusion

We first demonstrated the feasibility of a new type of tiled Ti:S crystal four-pass joule-level amplifier based on a 10-TW-level Ti:S CPA laser. Meanwhile, the redesign of the amplifier structure and the Ti:S crystal installation were used to solve some potential problems, including spectral modulation by slightly adjusting the crystal angle. We obtained the maximum output energy of 1.18 J with pump energy of 2.75 J, corresponding to the energy conversion efficiency of 35.3%. Ultimately, after the compressor, a pulse laser with a maximum peak power of 28 TW and pulse duration of 28.7 fs FWHM was achieved, and the combining efficiency of the two beams was 78.2% in a practical experiment. Due to similar energy conversion efficiency of the tiled Ti:S amplifier with that of the conventional single Ti:S amplifier, it could be used to replace the conventional Ti:S amplifier as a boost amplifier.

The tiled Ti:S crystals technology could suppress the PL of large-aperture Ti:S crystals, and the decrease of beam gap could further increase the focused intensity and combining efficiency. We will study the large-aperture tiled Ti:S amplifier to achieve PW-level or even higher peak power output and suppression of PL in the further experiments. Also, the tiling technology based on Ti:S crystals can be used to combine the tiling grating technology to further update the peak power and focused intensity in the CPA Ti:S lasers.

Acknowledgement

This work was supported by the National Key R&D Program of China (No. 2017YFE0123700), the Strategic Priority Research Program of the Chinese Academy of Sciences (No. XDB1603), the National Natural Science Foundation of China (No. 61925507), the Program of Shanghai Academic/Technology Research Leader (No. 18XD1404200), and the Shanghai Municipal Science and Technology Major Project (No. 2017SHZDZX02).

References

1. G. A. Mourou, T. Tajima, and S. V. Bulanov, "Optics in the relativistic regime," Rev. Mod. Phys. **78**, 309 (2006).
2. L. Volpe, R. Fedosejevs, G. Gatti, J. A. Pérez-Hernández, C. Méndez, J. Apiñaniz, X. Vaisseau, C. Salgado, M. Huault, S. Malko, G. Zeraouli, V. Ospina, A. Longman, D. De Luis, K. Li, O. Varela, E. García, I. Hernández, J. D. Pisonero, J. García Ajates, J. M. Alvarez, C. García, M. Rico, D. Arana, J. Hernández-Toro, and L. Roso, "Generation of high energy laser-driven electron and proton sources with the 200 TW system VEGA 2 at the Centro de Laseres Pulsados," High Power Laser Sci. Eng. **7**, e25 (2019).
3. R. Kodama, P. A. Norreys, K. Mima, A. E. Dangor, R. G. Evans, H. Fujita, Y. Kitagawa, K. Krushelnick, T. Miyakoshi, N. Miyanaga, T. Norimatsu, S. J. Rose, T. Shozaki, K. Shigemori, A. Sunahara, M. Tampo, K. A. Tanaka, Y. Toyama, T. Yamanaka, and M. Zepf, "Fast heating of ultra-high-density plasma as a step towards laser fusion ignition," Nature **412**, 798 (2001).
4. S. Fujioka, H. Takabe, N. Yamamoto, D. Salzmann, F. Wang, H. Nishimura, Y. Li, Q. Dong, S. Wang, Y. Zhang, Y. J. Rhee, Y. W. Lee, J. M. Han, M. Tanabe, T. Fujiwara, Y. Nakabayashi, G. Zhao, J. Zhang, and K. Mima, "X-ray astronomy in the laboratory with a miniature compact object produced by laser-driven implosion," Nat. Phys. **5**, 821 (2009).
5. D. Strickland and G. Mourou, "Compression of amplified chirped optical pulses," Opt. Commun. **56**, 219 (1985).
6. C. N. Danson, C. Haefner, J. Bromage, T. Butcher, J. C. F. Chanteloup, E. A. Chowdhury, A. Galvanauskas, L. A. Gizzi, J. Hein, D. I. Hillier, N. W. Hopps, Y. Kato, E. A. Khazanov, R. Kodama, G. Korn, R. X. Li, Y. T. Li, J. Limpert, J. G. Ma, C. H. Nam, D. Neely, D. Papadopoulos, R. R. Penman, L. J. Qian, J. J. Rocca, A. A. Shaykin, C. W. Siders, C. Spindloe, S. Szátmari, R. M. G. M. Trines, J. Q. Zhu, P. Zhu, and J. D. Zuegel, "Petawatt and exawatt class lasers worldwide," High Power Laser Sci. Eng. **7**, e54 (2019).
7. W. Q. Li, Z. B. Gan, L. H. Yu, C. Wang, Y. Q. Liu, Z. G. L. Xu, M. Xu, Y. Hang, Y. Xu, J. Y. Wang, P. Huang, H. Cao, B. Yao, X. B. Zhang, L. R. Cheng, Y. H. Tang, S. Li, X.Y. Liu, S. M. Li, M. Z. He, D. J. Yin, X. Y. Liang, Y. X. Leng, R. X. Li, and Z. Z. Xu, "339 J high-energy Ti:sapphire chirped-pulse amplifier for 10 PW laser facility," Opt. Lett. **43**, 5681 (2018).
8. Z. B. Gan, L. H. Yu, S. Li, C. Wang, X. Y. Liang, Y. Q. Liu, W. Q. Li, Z. Guo, Z. T. Fan, X. L. Yuan, L. Xu, Z. Z. Liu, Y. Xu, J. Lu, H. H. Lu, D. J. Yin, Y. X. Leng, R. X. Li, and Z. Z. Xu, "200 J high efficiency Ti:sapphire chirped pulse amplifier pumped by temporal dual-pulse," Opt. Express **25**, 5169 (2017)
9. F. Lureau, S. Laux, O. Casagrande, O. Chalus, A. Pellegrina, G. Matras, C. Radier, G. Rey, S. Ricaud, S. Herriot, P. Jougla, M. Charbonneau, P. A. Duvochelle, and C. Simon-Boisson, Proc. SPIE **9726**, 972613 (2016).
10. B. Le Garrec, D. N. Papadopoulos, C. Le Blanc, J. P. Zou, G. Chériaux, P. Georges, F. Druon, L. Martin, L. Fréneaux, A. Beluze, N. Lebas, F. Mathieu, and P. Audebert, Proc. SPIE **10238**, 102380Q (2017).
11. X. Liang, Y. Leng, C. Wang, C. Li, L. Lin, B. Zhao, Y. Jiang, X. Lu, M. Hu, C. Zhang, H. Lu, D. Yin, Y. Jiang, X. Lu, H. Wei, J. Zhu, R. Li, and Z. Xu, "Parasitic lasing suppression in high gain femtosecond petawatt Ti:sapphire amplifier," Opt. Express **15**, 15335 (2007).
12. F. Ple, M. Pittman, G. Jamelot, and J.-P. Chambaret, "Design and demonstration of a high-energy booster amplifier for a high-repetition rate petawatt class laser system," Opt. Lett. **32**, 238 (2007).
13. K. Ertel, C. Hooker, S. J. Hawkes, B. T. Parry, and J. L. Collier, "ASE suppression in a high energy titanium sapphire amplifier," Opt. Express **16**, 8039 (2008).
14. C. Peng, X. Liang, R. Liu, W. Li, and R. Li, "High-precision active synchronization control of high-power, tiled-aperture coherent beam combining," Opt. Lett. **42**, 3960 (2017).
15. R. Q. Liu, C. Peng, W. S. Wu, X. Y. Liang, and R. X. Li, "Coherent beam combination of multiple beams based on near-field angle modulation," Opt. Express **26**, 2045 (2018).
16. ELI—Extreme Light Infrastructure, White Book, http://www.elibeams.eu/wp-content/uploads/2011/08/ELIBook_neues_Logoedited-web.pdf.
17. G. Chanan, C. Ohara, and M. Troy, "Phasing the mirror segments of the Keck telescopes II: the narrow-band phasing algorithm," App. Opt. **39**, 4706, (2000).
18. G. J. Linford, B.C. Johnson, J. S. Hildum, W. E. Martin, K. Snyder, R. D. Boyd, W. L. Smith, C. L. Vercimak, D. Eimerl, and J. T. Hunt, "Large aperture

harmonic conversion experiments at Lawrence Livermore National Laboratory," App. Opt. **21**, 3633 (1982).
19. T. J. Zhang, M. Yonemura, and Y. Kato, "An array-grating compressor for high-power chirped-pulse amplification lasers," Opt. Commun. **145**, 367 (1998).
20. Y. Q. Liu, Y. X. Leng, X. M. Lu, Y. Xu, and C. Wang, "Irradiation uniformity at the Laser MegaJoule facility in the context of the shock ignition scheme," High Power Laser Sci. Eng. **2**, e8 (2014).
21. L. M. Frantz and J. S. Nodvik, "Theory of pulse propagation in a laser amplifier," J. Appl. Phys. **34**, 2346 (1963).
22. S. Tokita, M. Hashida, S. Masuno, S. Namba, and S. Sakabe, "0.3% energy stability, 100-millijoule-class, Ti:sapphire chirped-pulse eight-pass amplification system," Opt. Express **16**, 14875 (2008).
23. S. N. Bagayev, V. I. Trunov, E. V. Pestryakov, V. E. Leschenko, S. A. Frolov, and V. A. Vasiliev, "High-intensity femtosecond laser systems based on coherent combining of optical fields," Opt. Spectrosc. **115**, 311 (2013).
24. D. Wang and Y. X. Leng, "Simulating a four-channel coherent beam combination system for femtosecond multi-petawatt lasers," Opt. Express **27**, 36137 (2019).